DOI: https://doi.org/10.24297/jap.v15i0.8070

Preparation, Characterization and Antibacterial Efficiency of Olive Leaves Extract and Chitosan-Silver Nanoparticles using Electrochemical Method

M. T. Ahmed*, A. Sarhan, R. Hanie.

Polymer Research Group, Physics Department, Faculty of Science, Mansoura University, Mansoura, Egypt

moustf_1@yahoo.com

Abstract

The present work involves the improvement of chitosan-olive leaves extract and silver nanoparticles (Cs-OLE-AgNPs) using electrochemical approach followed by UV-irradiation reduction. The formation of silver nanoparticles (AgNPs) was characterized via UV–vis spectroscopy, Fourier transform infrared spectroscopy (FTIR), X-ray diffraction (XRD), differential scanning calorimetry (DSC), EDX, thermal gravimetric analysis (TGA) and Swelling. The obtained nanoparticles average size was 36.19 nm. UV Spectroscopy show increase of peaks at 320 and 345 nm indicate the formation of a large cluster of AgNPs. Cs-OLE and Cs-OLE-AgNPs also demon started a relativity high antibacterial against both Escherichia coli (E. coli) and Staphylococcus aureus (S. aureus) bacteria. AgNPs show broadspectrum antibacterial activity at lower concentration (0.56%) and may be a regarded as a good alternative therapeutic approach in the future.

Keywords: Chitosan, Olive leaves extract, Silver nanoparticles, Antibacterial activity. Electrochemical method.

Introduction

Chitosan is a linear polysaccharide comprises of β-(1→4)-2-acetamido-D-glucose and β-(1→4)-2-amino-D-glucose units obtain by alkaline deacetylation of chitin which is the second most abundant organic compound beside cellulose. Chitosan has three type of function group's free amino acid, hydroxyl andacetamide group, which influence the solubility of the polymer. Chitosan has proven to be non-toxic, biodegradable, biocompatible and has an antimicrobial characteristic, so it has variety application in the medicalfields such as antitumor, wound healing and hypercholesterolemia treatment [1-3].

Olive tree leaves consider agriculture waste, which contains flavonoid and large concentration of phenolic acid, of which oleuropein is most abundant [4]. Olive leaves have benefit in the treatment of conditions caused by virus, bacterium andprotozoan because it has antimicrobial activity, antioxidant properties, anti HIV properties, vasodilatation effect, hypoglycemic effect and anticancer properties [5-7].

The recent study has concentrated recently on analysis and improvement of nanoparticles (Ag, Au, Pt and Pd) owing to their uncommon properties and potential applications in various fields including magnetic, optical, catalytic, electrical, and sensing technologies compared to bulk metals [8].

Silver nanoparticles are one of the most universal antibacterial substances, which low concentration of it gives high antibacterial activity [9]. Applications have been found for silver nanoparticles in wide range fields from electronic, antimicrobial to diagnostics and therapeutics [10].

The inexperienced synthesis technique (the electrochemical method) delineate within the gift the gift study doesn't solely represents a cheap and comparatively fast technique for developing Cs-OLE-AgNPs, however, it's additionally provide varied benefits of biocompatibility and ecofriendliness for various biological applications as all the materials utilized in the work square measure renewable and environmentally benign.

The goals of the present study are to improve a film of (Cs-OLE) and (Cs-OLE-AgNPs) and investigate characterization, antibacterial and thermal difference between them. The major aim of this study focuses on the study the change of antibacterial activity against Escherichia coli (E. coli) and Staphylococcus aureus (S. aureus) happen owing to adding silver nanoparticles by the electrochemical method to chitosan-olive leaves extract.

Experimental and method

Materials

Chitosan powder (degree of deacetylation of 93%) was obtained from Oxford laboratory reagent (Thani, India). Tween, glycerol, ethanol and acetic acid (EL-Naser pharamatical chemical Egypt Co. Silver plate (20 × 40 × 5) mm with purity 99.99%, were provided by Sigma-Aldrich (St Louis, USA). The Ag sheet was used as the anode in the cell, polished by victimization fine abrasive, clean by dimethyl ketone, ethyl alcohol (90 %) and de-ionized water. Platinum sheet (20 × 40 × 2) mm obtained from Sigma, were used as the cathode. De-ionized water was utilized for all the samples preparation.

Method

Preparation of olive leaves extract

The dried olive leaves powder using a mixer grinder and 200 g portions of finely olive leaves was mixed with 80% ethanol for 2 h at 60 °C then use Ultrasonic bath for 10min, The extracts were through filter paper (Waterman No. 1) and afterwards dried overnight in an electric oven at 50 °C in order to form crude. Finally, this crude was stored at 4 °C until further analysis.

Synthesis of chitosan and olive leave extract film

Cs solution prepared with 1% (w/w) Cs in 1% (w/w) acetic acid at room temperature (T= 30 ^{o}C) and After overnight stirring, the solution filters in order to remove any traces and impurities. Then, glycerol (glycerol/chitosan = 0.5, w/w) and Tween 80 at 0.5% (w/w) were blended and stirred for 30 min. Then, olive leaves extract was added to the chitosan solution (10g/l) with stirring overnight and use centrifuge (1500rps) to remove any insoluble particles. The solution poured into glass Petri dishes and put in the oven at 50 ^{o}C for 24 h.

Preparation of chitosan-olive leaves extract and silver nanoparticles

Cs-OLE-AgNPs were obtained using electrochemical oxidation /complexation method by using a constant potential equal 1.4 V for 2 h. The cell comprises of 5 cm-separated Ag (anode) and Pt (cathode) sheets. These two electrodes were immersed with in the electrolytic solution (Cs-OLE) via (Pt) platinum wires that sealed to a glass tube followed by UV Irradiation reduction (λ_{max} = 254 nm at 30 ^{o}C for 1h) [11].

Instrumentation

The UV-Vis spectra of the Cs, Cs-OLE and Cs-OLE-AgNPs measured in the range of 200-600 nm utilizing ATI Unicom UV-Vis. Spectrophotometer. The measurements completed at room temperature using quartz cuvettes and the blank is 100 ml water and 1 ml acetic acid. The FTIR spectra of the Cs, OLE, Cs-OLE and Cs-OLE-AgNPs were measured in range (400–4000) cm^{-1} using a Mattson 5000 FTIR spectrometerat 303 Kwith resolution of 8 cm^{-1}. All sample place in the sample holder of the spectrometer. The X-ray diffraction patterns (XRD) of the Cs, Cs-OLE and Cs-OLE-AgNPs samples obtain utilize Philips PW 1390 X-ray diffractometer. The X-ray diffraction provides with a beam monochromatic and CuKα radiation at λ =1.5406 A°. The applied voltage was 40 KV and the current intensity was 40 mA. Sec. The (2θ) angle was scanned in the range of 4^{o} to

70°, and the X-ray runs were applied at a scanning speed of 2θ=2°/min. DSC analysis carries out using a NETZSCH STA 409C/CD instrument,samples place into an aluminum pan then scale with a crimped lid and heat from 20 °C to 800 °C at a rate of 10°C/min with Him as carrier gas at a flow rate (50 ml/min). It was worked in the metallurgical institute (El-Tebbeen Helwan). Thermo gravimetric analyses achieved with rate of heating at 10°C/min.

Swelling studies

The ensuing Cs-OLE and Cs-OLE-AgNPs complexes method caste in 10 cm Petri dishes and dry at temperature, then followed by drying at 50°C for 1days. The samples (3x4) cm, then cut from the pure metal, Cs-OLE and Cs-OLE-AgNPs samples. The thickness of the samples was existed within vary of 250-300 µm employing micrometer. The swelling behavior was studied by sinking the weighted samples in de-ionized water at temperature for planned periods. The weighted samples were set as operate of your time once drying it exploitation paper to get rid of water drops. The swelling of the samples was expressed because the siharevainglorous (S%) as shown in the next equation.

$$S\% = [(W_s - W_d)/W_d] \times 100$$

Where W_d is the weight of the dry film (g) and W_s is the weight of the swelled film at time t.

Antibacterial assay

Clinical isolates

Two identified clinical isolates particularly coccus aureus (S. aureus) and Escherichia coli (E. coli) provide from biological science department, faculty of Agriculture, Mansoura University. All microorganism clinical isolates maintain habitually on culture medium slants (Oxide) at 4 °C.

Preparation of bacterial inoculum

Twenty-fourhour nutrient broth cultures of take a look at microorganism to grow in associate orbital shaking brooder, centrifuge, wash doubly with PBS and so standardize to about 106 CFU ml victimisation broth medium.

Bacterial sensitivity test

Standard well agar diffusion methodology carries bent on find the activity of Cs-OLE and Cs-OLE-AgNPs against the clinical microorganism isolates in step with Cheesbrough (2000) [12]. For antibacterial drug activities of the compounds, wells build in plates contain culture medium seed with one hundred µl of twenty-four hour of every clinical isolate. The plates were left in icebox for two hour afterwards, incubated at 37 °C for twenty-four hour. The diameter of inhibition zones was measured and tabulated.

Result and Discussion

Fourier transform infrared spectroscopy (FTIR).

FT-IR spectroscopy use to confirm the crosslinking reaction between Cs-OLE and Cs-OLE-AgNPs. Figure1. (a) shows FTIR spectra of chitosan (Cs) which show abroad band at 3445 cm^{-1} which is attribute to O-H (hydroxyl group) and NH_2 (amine group), sharp peaks at (2923-2854) cm^{-1} which attributed to symmetric and asymmetric C-H and peaks appear at (1656, 1550, 1422, 1252 and 1034) cm^{-1} refer to C=O, N-H bending (amideⅡ), aromatic ring, C-O-H and C-O stretching [13, 14]. For olive leaves extract (OLE) the broadband at 3425 cm^{-1} attribute to O-H (hydroxyl group), sharp peak at 2929cm^{-1} correspond to C-H stretching band and

the peaks appear at (1694, 1629 and 1452) cm^{-1} refer to C=O of lactones, ketones or carboxylic anhydrides, C-O stretching vibration in quinine and C=C aromatic ring [15]. The main difference between Cs and Cs-OLE is broad and shift of OH peak and other peaks appear at 1656 and 1550 cm^{-1} to 1634 and 1547 cm^{-1} indicate the presence of interaction between OLE and Cs [16]. For Cs-OLE-AgNPs there's shift and decrease in strength of peaks 1547 and 1634 cm^{-1} to 1565 and 1646cm^{-1} happen due to binding of AgNPs with N-H or COO^{-}. And finally disappear of the peak at (1415, 1159 and 655) cm^{-1} happen due to increasing in Ag^{+} ion observation so there's good interaction between polymer and silver nanoparticle [17, 18], After 1 hirradiation as shown in figure.2 (b) hydrogen peak at 3440 shifts to 3446 cm^{-1}, minor broadening and peak at 890 cm^{-1} suggested that there was good interaction between AgNPs and Cs-OLE [19].

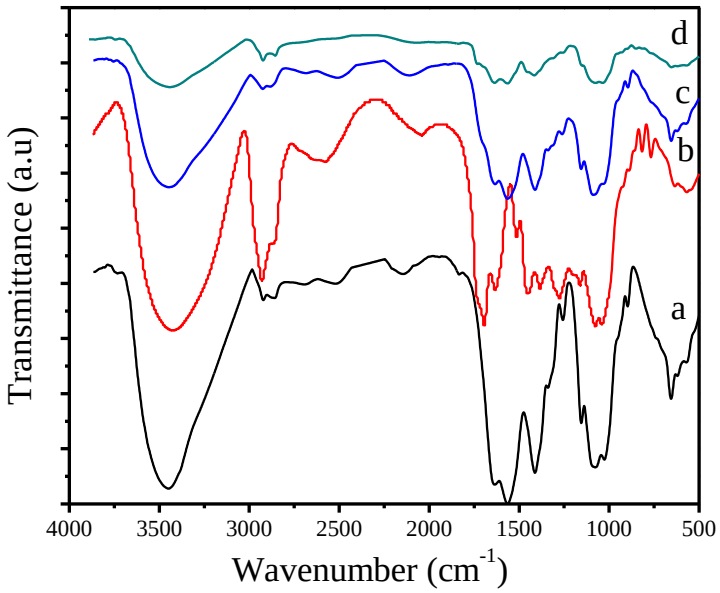

Figure 1. FT-IR spectra of (a) Cs, (b) OLE, (c) Cs-OLE and (d) Cs-OLE-AgNPs.

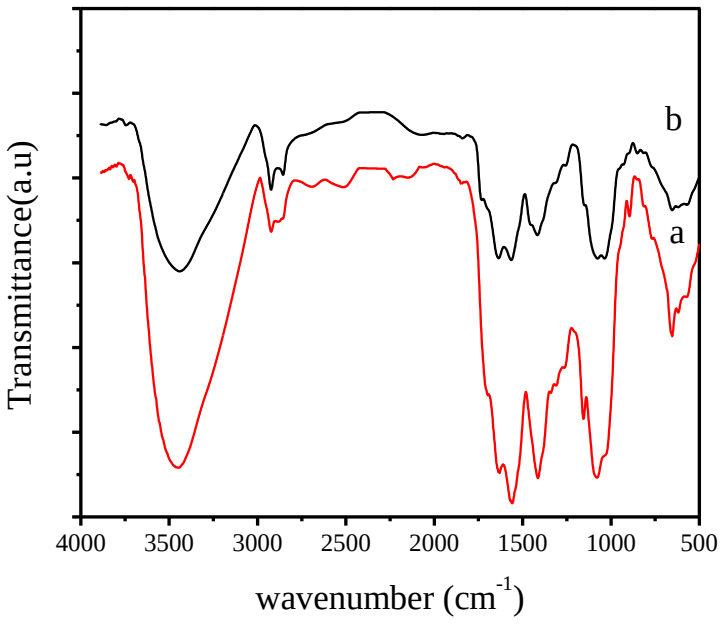

Figure 2. FT-IR spectra of (a) Cs-OLE-AgNPs and b) Cs-OLE-AgNPs after 1h radiation.

UV Spectroscopy

UV spectroscopy for Cs shows two peaks at 213 and 243 nm which happen occur attributed to π-system of benzene ring [20]. By adding OLE to Cs the peak at 243 nm shifted to 251 nm and other peaks appear at 275, 320,345 nm refer to OLE. In figure.3 λ_{max} shift from 243 to 320 nm and energy gap decrease from 5.10 to 3.87eV, so chitosan and olive leave extract have lower energy difference, more conjugated system and more stable than chitosan. All of this indicates the presence of good interaction between chitosan and extract. In figure.3(c) by using electrochemical method to add AgNPs to Cs-OLE solution, there's increase in absorption of peaks at 320 and 345nm refer to formation of large cluster of silver nanoparticles and this may occur as a result of chitosan and olive leaves extract solution acidity (PH=4.1), so this may be lead to strong reducing power [21, 22]. In figure. 4 there is an increase in all peaks absorption after 1 h of irradiation which suggests that expose the sample to UV irradiation leads to enhancement of interaction between chitosan, olive leave extract and silver nanoparticle (Cs-OLE-AgNPs).

As shown in the table energy gap can be calculated by this equation

$$Energy\ (E)\ =\ [\ Planks\ Constant\ (h)\ \times Speed\ of\ Light\ (C)]\ /\ Wavelength\ (\lambda)$$

Where, E = Bandgap, h = Planks constant (6.626×10^{-34} J. s), C = Velocity of Light (2.99×10^{8} m/s) and λ = Absorption peak value. Also, 1eV = 1.6×10^{-19} J (Conversion factor).

The band gap can be estimated easily by this formula [23].

Table 1. UV maximum peak and energy gap for Cs, Cs-OLE and Cs-OLE-AgNPs.

Sample	Max wave length (nm)	Energy gap (eV)
Cs	243	5.10
Cs-OLE	320	3.87
Cs-OLE-AgNPs	345	3.59

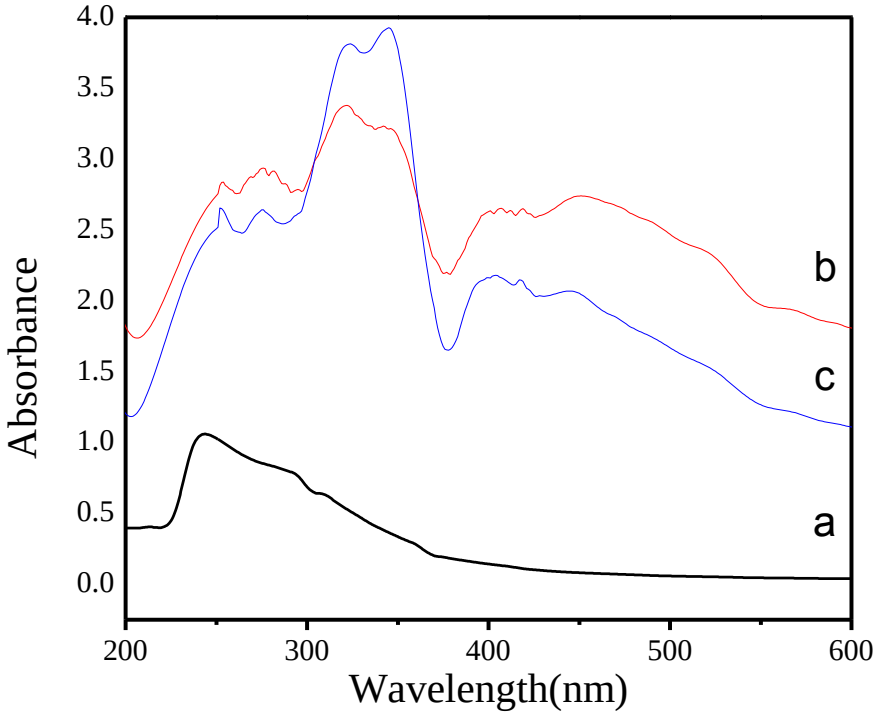

Figure 3. UV-Vis spectra of (a) Cs, (b) Cs-OLE and (d) Cs-OLE-AgNPs.

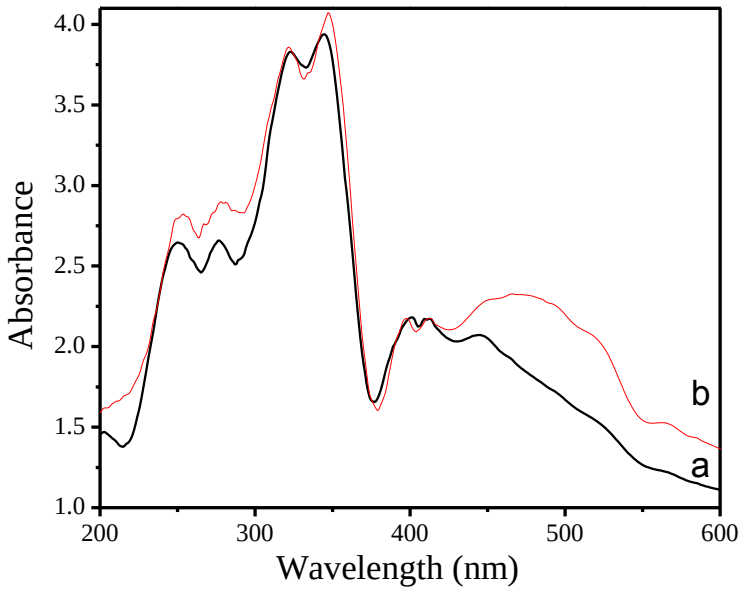

Figure 4. UV-Vis spectra of (a) Cs-OLE-AgNPs and b) Cs-OLE-AgNPs after 1h radiation.

X-ray diffraction (XRD)

XRD in figure 5 (a) shows chitosan have four peaks weak at$2\theta^{o}$ of 8.08^{o}, 11.47^{o}, 18.17^{o} and 22.53^{o} with a degree of crystallinity equal 26.21% this degree increases for chitosan and olive leave extract to 30.99% and increase again for Cs-OLE-AgNPs to 46.96% [3]. On the other hand, compare the diffractogram of Cs-OLE and

Csshow that various peaks in Cs disappear in CS-OLE diffractogram. Using an electrochemical method to add AgNPs to Cs-OLE solution sharp peaks appear at 27.77°, 32.16°, 46.19°, 54.75°, 57.59°, and 76.7° which indicate the presence of silver nanoparticles [24]. In additions these peaks may be contributing to (111), (200), (220), (311), (222) and (311) crystallographic planes.

Calculate the crystal size of AgNPs at each peak as shown in table 2 and the average crystal size of silver nanoparticle which equal 36.8 nm by Scherrer equation,

$$D = n\lambda/\beta cos\theta$$

where D is the crystallite size, n is a constant (=0.9, when the particles are spherical), λ is the wavelength, β is the line width (obtained after correction for the instrumental broadening) and θ is the diffraction angle [25].

Table 2. shows the AgNPs crystal size at each peak position.

Position of the Peak (2ɵ)	Crystal size of AgNPs
27.7751	35.95
32.1688	38.72
46.1903	21.53
54.7526	18.09
57.59	95.22
76.7428	7.63

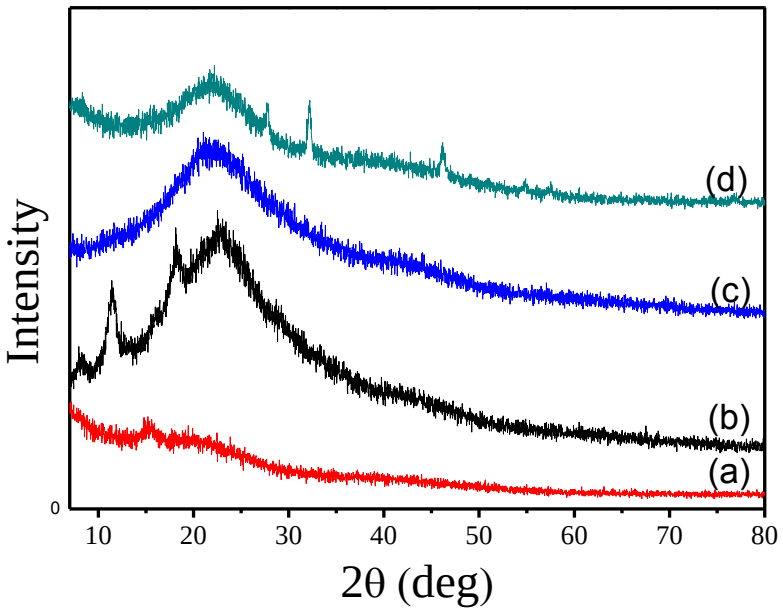

Figure 5. XRD Pattern for (a) OLE, (b) Cs, (c) Cs-OLE and (d) Cs-OLE-AgNPs.

Differential scanning calorimetry (DSC)

DSC in the figure.6 (a) shows that first peak at 125 ^{o}C may be ascribed to loss of water while the second peak at 285^{o}C related to decomposition of amine. For (b) and (c) show that water holding capacity of Cs-OLE is higher than Cs-OLE-AgNPs, this means there's good interaction happen between Cs-OLE and AgNPs. At Cs-OLE sample the peak appears at 45 ^{o}C is due to water evaporation and the glass transition temperature T_g equal 106 ^{o}C. Due to increase crystallinity degree of Cs-OLE-AgNPs the glass transition temperature T_g cannot be indicated [26].

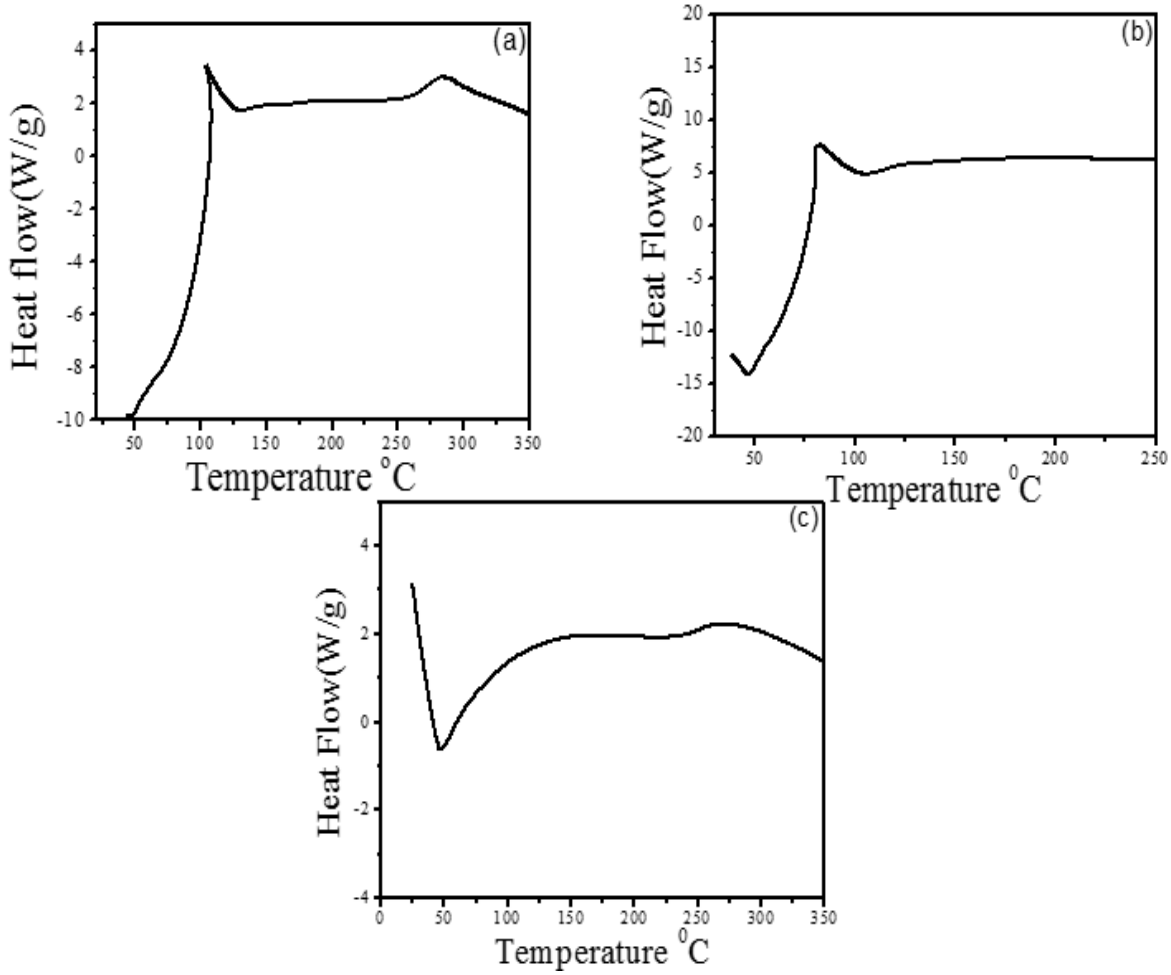

Figures 6. DSC curves of (a) Cs, (b) Cs-OLE and (c) Cs-OLE-AgNPs.

Thermal Gravimetric Analysis (TGA)

Thermal gravity (TG) is the branch of thermal analysis which investigates the mass change of sample as a function of temperature in scanning mode. The thermal decomposition curves provide as the inflection points depict the peak maximum to determine the degradation characteristics (Table 3). Simultaneously, percentage mass loss during thermal decomposition investigates (Table 4) [27].

As shown in the figure 7 there are multistage of decomposition of Cs-OLE and Cs-OLE-AgNPs sample. The thermal decomposition from 100 to 700^{o}C may be attributed to desorption of bioorganic compounds. For Cs-OLE the first stage at 58.3^{o}C and second stage at 72.92^{o}C of decomposition is occurring due to loss of volatile component. The third stage of decomposition at 267.56^{o}C with major loss weight 32.01% correspond to decomposition of polymer or deacetylation of chitosan chain [27, 28]. Add AgNPs to Cs-OLE lead to shift of

first, third, fourth stages and disappear of the second stage as a result of decreasing water holding capacity. The high of weight loss indicates that the bio-organic material crystallizes with AgNPs [29]. The thermal decomposition of the sample contained silver is faster than sample without silver at 800°C the residues mass equal 29.181%.

Table 3. Thermal decomposition temperature (based on inflection points) of Cs-OLE and Cs-OLE-AgNPs.

Sample	Inflection point1 ^{0}C	Inflection point2 ^{0}C	Inflection point3 ^{0}C	Inflection point4 ^{0}C
Cs-OLE	58.33	77.92	267.56	425.36
Cs-OLE-AgNPs	52.69	ND	266.22	416.66

Table 4. Percentage mass loss and residue of Cs-OLE and Cs-OLE-AgNPs

Sample	Mass loss1 %	Mass loss2 %	Mass loss3 %	Mass loss4 %	Final residue %
Cs-OLE	9.285	32.01	12.70	13.41	32.5
Cs-OLE-AgNPs	11.12	38.75	15.13	5.839	29.181

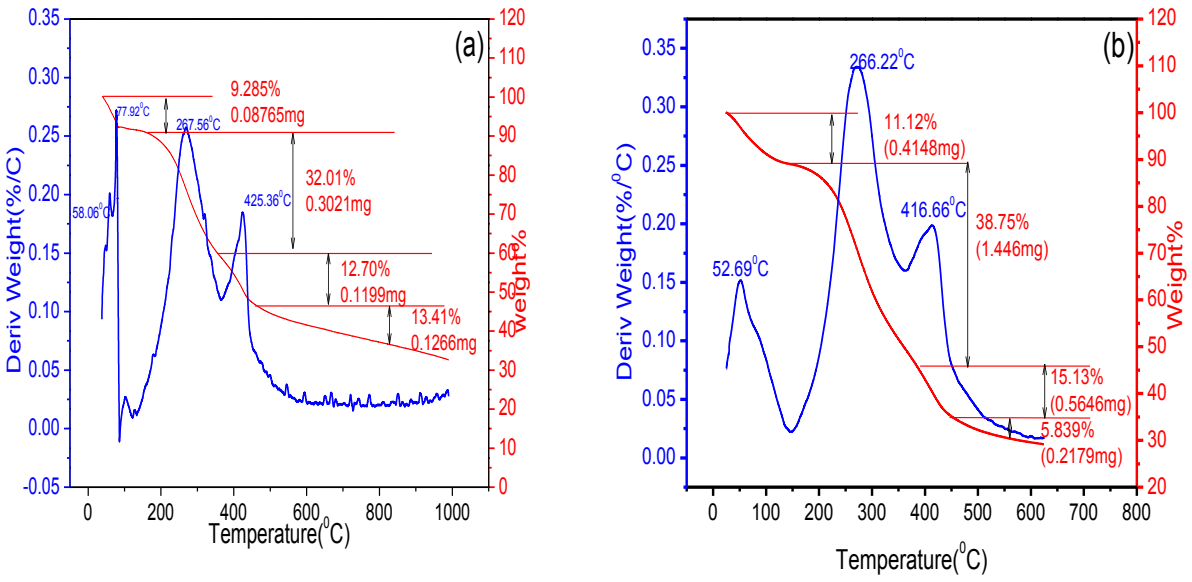

Figures 7. Thermal decomposition curves of (a) Cs-OLE and (b) Cs-OLE-AgNPs.

Antibacterial assay

Silver nanoparticles AgNPs have high antibacterial activity. The antibacterial activity of different samples demonstrates that both gram -positive and gram-negative bacteria were inhibited by a various solution. The results of the antibacterial activity are depicting in (table 5 and figure 8).

Table 5. shows antibacterial efficiency appeared as the inhibition zone diameter (mm)

Sample	E. coli	S. aurous
Cs	ND	2
OLE	ND	1
Cs-OLE	8	10
Cs-OLE-AgNPs	12	15

Figure 8. Shows antibacterial efficiency appeared as the inhibition zone .

Sample	OLE	Cs	Cs-OLE	Cs-OLE-AgNPs
S. aurous		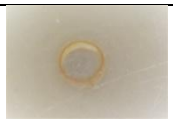	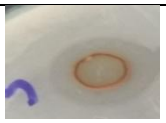	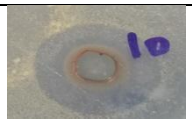
E. coli		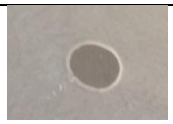		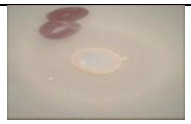

The mechanism of antibacterial of solutions may be occur as result of interaction with lipophilic components of the bacterial membrane, which may cause varies in H^+ and K^+ permeability, and lastly, destroy the main functions and lead to death of the cell.

In addition, the antibacterial activity against S.aureus in the solution incorporated with 10 g/L OLE was remarkable higher than that incorporated with chitosan or extract alone, suggesting that there is a synergistic action.

Adding silver nanoparticle to chitosan and olive leaves extract solution by Electrochemical, the ability of chitosan, olive leaves extract and silver nanoparticles to inhibit growth greater than chitosan and olive leaves extract.

Generally, gram-positive bacteria (S.aureus) consider more sensible than gram-negative bacteria (E. coli) to antibacterial compounds [30, 31].

Swelling

The swelling behavior of chitosan, chitosan and olive leave extract and chitosan, olive leave and silver nanoparticle are obtained as shown in figure 9 by adding olive leave to chitosan then silver nanoparticle by the electrochemical method to sample the swelling ratio decrease this may be happen due to crosslinking with chitosan [11]. This result agrees with water capacity from DSC result.

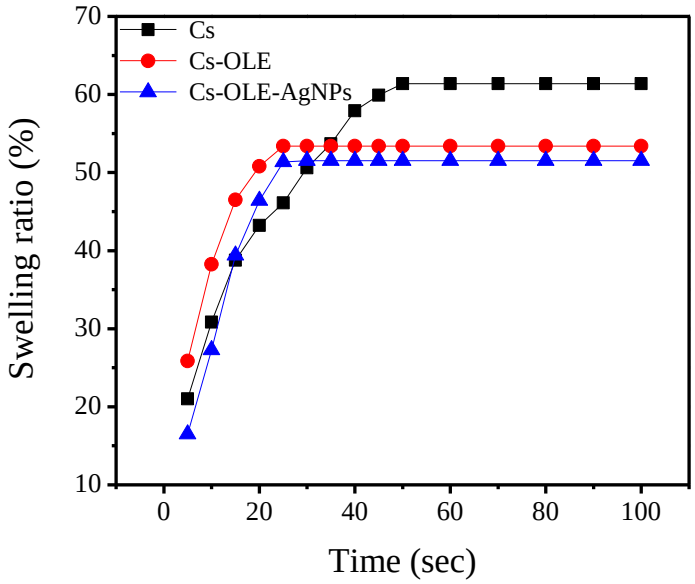

Figure 9. Swelling patterns of CS, Cs-OLE and Cs-OLE-AgNPs films.

Conclusion

FTIR, UV Spectroscopy and XRD prove that there's good interaction between Chitosan- Olive leaves extract and silver nanoparticles. Expose Cs-OLE-AgNPs to UV irradiation for 1 h enhance the interaction between the components. Large clusters of AgNPs synthesis using Cs-OLE solution with average size 36.1 nm by an electrochemical method for 2 h. Cs-OLE and Cs-OLE-AgNPs also demon started a relativity high antibacterial activity against E- coli and S- aureus bacteria. Low concentration of AgNPs (0.56%) of sample increase inhibition zone and this is a small amount.

References

1. Bui, V., Park, D., and Lee, Y.-C., Chitosan combined with ZnO, TiO2 and Ag nanoparticles for antimicrobial wound healing applications: a mini review of the research trends, Polymers, (2017) 9 (1), 21.

2. Wenshui, X., Ping, L., Talba, T., Wenxiu, G., and Bo, L., Chitosan Modification and Pharmaceutical, Biomedical Applications Drugs, (2010), 8, 1962-1987.

3. Acosta, N., Sánchez, E., Calderón, L., Cordoba-Diaz, M., Cordoba-Diaz, D., Dom, S., and Heras, Á., Physical stability studies of semi-solid formulations from natural compounds loaded with chitosan microspheres, (2015), Marine drugs, 13 (9), 5901-5919.

4. Goldsmith, C. D., Vuong, Q. V., Stathopoulos, C. E., Roach, P. D., and Scarlett, C. J., Optimization of the aqueous extraction of phenolic compounds from olive leaves, Antioxidants, (2014), 3 (4), 700-712.

5. De Leonardis, A., Aretini, A., Alfano, G., Macciola, V., and Ranalli, G., Isolation of a hydroxytyrosol-rich extract from olive leaves (Olea Europaea L.) and evaluation of its antioxidant properties and bioactivity, European Food Research and Technology, (2008), 226 (4), 653-659.

6. Fares, R., Bazzi, S., Baydoun, S. E., and Abdel-Massih, R. M., The antioxidant and anti-proliferative activity of the Lebanese Olea europaea extract, Plant Foods for Human Nutrition, (2011), 66 (1), 58-63.

7. Goldsmith, C. D., Vuong, Q. V., Sadeqzadeh, E., Stathopoulos, C. E., Roach, P. D., and Scarlett, C. J., Phytochemical properties and anti-proliferative activity of Olea europaea L. leaf extracts against pancreatic cancer cells, Molecules, (2015), 20(7), 12992-13004.

8. He, J., Kunitake, T., and Nakao, A., Facile in situ synthesis of noble metal nanoparticles in porous cellulose fibers, Chemistry of Materials, (2003), 15 (23), 4401-4406.

9. Omrani, A. A., and Taghavinia, N., Photo-induced growth of silver nanoparticles using UV sensitivity of cellulose fibers, Applied Surface Science, (2012), 258 (7), 2373-2377.

10. Mittal, A. K., Kaler, A., and Banerjee, U. C., Free Radical Scavenging and Antioxidant Activity of Silver Nanoparticles Synthesized from Flower Extract of Rhododendron dauricum, Nano Biomedicine and Engineering, (2012), 4 (3).

11. Reicha, F. M., Sarhan, A., Abdel-Hamid, M. I., and El-Sherbiny, I. M., Preparation of silver nanoparticles in the presence of chitosan by electrochemical method, Carbohydrate polymers, (2012), 89 (1), 236-244.

12. Cheesbrough, M, District laboratory practice in tropical countries: Cambridge university press, (2006).

13. Romainor, A. N. B., Chin, S. F., Pang, S. C., and Bilung, L. M., Preparation and characterization of chitosan nanoparticles-doped cellulose films with antimicrobial property, Journal of Nanomaterials, 2014, 130.

14. Altiok, D., Altiok, E., and Tihminlioglu, F., Physical, antibacterial and antioxidant properties of chitosan films incorporated with thyme oil for potential wound healing applications, Journal of Materials Science: Materials in Medicine, (2010), 21 (7), 2227-2236.

15. Silverstein, R. M., Bassler, G. C., and Morrill, T. C., Spectrometric identification of organic compounds, New York: Wiley, 1981, 4th ed.

16. Khalil, M. M., Ismail, E. H., El-Baghdady, K. Z., and Mohamed, D., Green synthesis of silver nanoparticles using olive leaf extract and its antibacterial activity, Arabian Journal of Chemistry, (2014), 7 (6), 1131-1139.,

17. Ali, S. W., Rajendran, S., and Joshi, M., Synthesis and characterization of chitosan and silver loaded chitosan nanoparticles for bioactive polyester, Carbohydrate polymers, (2011), 83 (2), 438-446.

18. Kaur, P., Choudhary, A., and Thakur, R., Synthesis of chitosan-silver nanocomposites and their antibacterial activity, Int J Sci Eng Res, (2013), 4 (4), 869.

19. Ismail, E. H., Khalil, M. M., Al Seif, F. A., El-Magdoub, F., Bent, A., Rahman, A., and Al, U., Biosynthesis of gold nanoparticles using extract of grape (Vitis vinifera) leaves and seeds, Prog Nanotechnol Nanomater, (2014), 3, 1-12.

20. Yin, Y., Dang, Q., Liu, C., Yan, J., Cha, D., Yu, Z., Cao, Y., Wang, Y., and Fan, B., Itaconic acid grafted carboxymethyl chitosan and its nanoparticles: preparation, characterization and evaluation, International journal of biological macromolecules, (2017), 102, 10-18.

21. de Barros Santos, E., Madalossi, N. V., Sigoli, F. A., and Mazali, I. O., Silver nanoparticles: green synthesis, self-assembled nanostructures and their application as SERS substrates, New Journal of Chemistry, (2015), 39 (4), 2839-2846.

22. Linnert, T., Mulvaney, P., Henglein, A., and Weller, H., Long-lived nonmetallic silver clusters in aqueous solution: preparation and photolysis, Journal of the American Chemical Society, (1990), 112 (12), 4657-4664.

23. Anderson, R. J., Bendell, D. J., and Groundwater, P. W., Organic spectroscopic analysis: Royal Society of Chemistry, (2004), (Vol. 22).

24. Loo, Y. Y., Chieng, B. W., Nishibuchi, M., and Radu, S., Synthesis of silver nanoparticles by using tea leaf extract from Camellia sinensis. International journal of nanomedicine, (2012), 7, 4263.

25. Azaroff, L. V., and Azároff, L. V., Elements of X-ray Crystallography: McGraw-Hill New York, (1968), (Vol. 610).

26. Haerudin, H., Pramono, A. W., Kusuma, D. S., Jenie, A., Voelcker, N., and Gibson, C., Preparation and characterization of chitosan/ontmorillonite MMT nanocomposite systems, (2010).

27. Pereira, F. S., da Silva Agostini, D. L., Job, A. E., and González, E. R. P., Thermal studies of chitin–chitosan derivatives, Journal of thermal analysis and calorimetry, (2013), 114 (1), 321-327.

28. Neto, C. D. T., Giacometti, J. A., Job, A. E., Ferreira, F. C., Fonseca, J. L. C., and Pereira, M. R., Thermal analysis of chitosan based networks, Carbohydrate Polymers, (2005), 62 (2), 97-103.

29. Francis, L., Balakrishnan, A., Sanosh, K. P., and Marsano, E., Hydroxy propyl cellulose capped silver nanoparticles produced by simple dialysis process, Materials Research Bulletin, (2010), 45 (8), 989-992.

30. Kaur, P., Choudhary, A., and Thakur, R., Synthesis of chitosan-silver nanocomposites and their antibacterial activity, Int J Sci Eng Res, (2013), 4 (4), 869.

31. Cao, X. L., Cheng, C., Ma, Y. L., and Zhao, C. S., Preparation of silver nanoparticles with antimicrobial activities and the researches of their biocompatibilities. Journal of Materials Science: Materials in Medicine, (2010), 21 (10), 2861-2868.